Available online at www.sciencedirect.com
SCIENCE DIRECT®
International Journal of Mass Spectrometry 241 (2005) 173–184
International Journal of Mass Spectrometry
www.elsevier.com/locate/ijms

Dynamical control of 'statistical' ion–molecule reactions

Jianbo Liu, Scott L. Anderson*

Department of Chemistry, University of Utah, 315 South 1400 East, Room 2020, Salt Lake City, UT 84112-0850, USA

Received 11 November 2004; accepted 7 December 2004

Abstract

Experimental and theoretical studies of two ion–molecule reactions are reviewed. The reactions of H_2CO^+ and $C_2H_2^+$ with methane are both mediated by long-lived complexes at low collision energies. The complex lifetimes, product recoil energy and angular distributions, and product branching ratios are all in good agreement with predictions based on statistical decay of the intermediate complexes. Nonetheless, it is clear that both reactions are, in fact, controlled by dynamical effects. In particular, reactivity is strongly and mode-specifically dependent on the vibrational state of the reactants, whereas a statistical mechanism would depend only the energy content of the vibrations. The vibrational effects reflect the dynamics involved in the formation and decay of weakly bound precursor complexes, before the collisional interaction can scramble the initial state information.

Keywords: Ion–molecule reaction dynamics; Vibrational effects; Precursor complex

1. Introduction

Many ion–molecule reactions are assumed to go via mechanisms mediated by intermediate complexes, ranging from simple electrostatically or hydrogen-bonded species, to covalently bonded complexes. Evidence for the role of complexes includes isotopic scrambling, forward–backward symmetric product angular distributions, and product branching and recoil energies consistent with statistical unimolecular decay of a long-lived intermediate. In such reactions, it is safe to say that the break up of the complex is a statistical process, i.e., depends only on the total energy and angular momentum of the complex. In this paper, we use two examples of such reactions to make the point that even for reactions mediated by a statistical complex, the reaction may be controlled by dynamics, i.e., the rate-limiting step depends sensitively on the details of reactant preparation, not simply on energy and angular momentum.

It is useful to review behavior expected for a reaction under purely statistical control. The fundamental assumption in statistical reaction models is that energy is randomized, i.e., distributed statistically among all the energetically accessible states of the system. For statistical factors to control reaction, this randomization must occur prior to the rate-limiting step in the mechanism [1–3]. Inherent in this assumption is the requirement that energy exchange between different degrees of freedom be facile, so that energy randomization can be rapid compared to the reaction time. The rate of a particular process (e.g., breakup of a complex, or interconversion between different complex isomers) is proportional to the total number of energetically accessible states (subject to angular momentum conservation) at the transition state (TS). As a consequence, statistical reactions tend to occur by paths close to the minimum energy path, as the density of states is highest for such paths [4].

A typical approach to predicting behavior expected for a statistical mechanism involves calculating the energies, moments of inertia, and vibrational frequencies for the complexes and transition states connecting reactants to various product channels. For many ion–molecule reactions, there are no energy barriers for approach of reactants, thus it is assumed that the initial ion–molecule complex forms efficiently. A transition-state-theory-based model such as the

* Corresponding author. Tel.: +1 801 585 7289; fax: +1 801 581 8433.
E-mail address: anderson@chem.utah.edu (S.L. Anderson).

1387-3806/$ – see front matter © 2004 Elsevier B.V. All rights reserved.
doi:10.1016/j.ijms.2004.12.010

Rice–Ramsperger–Kassel–Marcus (RRKM) theory [5,6] or phase space theory [1] is then used to calculate the unimolecular rates for crossing the various transition states (TSs) leading from this initial complex to other complexes and to various product channels (including dissociation back to reactants). The product branching is given by the ratio of the rates, and recoil energy distributions can also be calculated based on the assumption of statistical energy partitioning in the products. This basic approach has been successful in accounting for many experimental observations [1], and these successes support the assumptions made in the statistical models.

However, advances in both experiment and theory have allowed more detailed investigations of dynamical effects on chemical reactions, leading to reconsideration of the validity of the fast energy exchange assumption inherent in the statistical approach [7]. Theoretically, for example, by using ab initio direct dynamics trajectory simulation, Hase and coworkers [8], and Ammal et al. [9], have recently demonstrated that reacting molecules do not necessarily follow the minimum energy pathway when kinetic energy is accounted for, and discussed these phenomena in terms of relationship between intra-molecular vibrational redistribution (IVR) and molecular structure. Experimentally, non-statistical effects have been seen in the variation of unimolecular lifetime with energy [10,11], in product energy distributions [12,13], product branching ratios [14], and in the effects of electronic [15] and vibrational excitation [16].

Here we focus on two systems which appear statistical to all the usual experimental probes, i.e., statistical decay of complexes adequately accounts for complex lifetimes, product branching ratios, angular and recoil energy distributions, etc. Nonetheless these "statistical" reactions are clearly controlled by dynamical effects, as shown by strong dependence of reactivity on the details of reactant preparation. These effects are observed in experiments where vibrationally mode-selected ions are reacted under conditions where both integral and differential cross-sections can be measured over a wide range of collision energy (E_{col}) [17–19]. When, as we almost always observe, reactivity depends on vibrational mode, not simply on vibrational energy, the implication is that the rate-limiting step in the mechanism is under dynamical control. The goal of this paper is to show how dynamical effects fit into otherwise statistical reaction mechanisms, and to point out the type of systems where dynamical effects are likely to be important. We believe that such systems are, in fact, quite common.

2. Experimental and computational methods

The experimental methodology has been described in detail previously [20]. The most difficult aspect of the method is preparing polyatomic cations with controlled excitation in different vibrational modes. Depending on the system, we have been successful with both resonance-enhanced multiphoton ionization (REMPI) and mass-analyzed threshold ionization (MATI) [21].

The general considerations for successful REMPI state selection have been outlined previously [18]. In brief, the neutral precursor molecules are excited by one or more photons to an intermediate electronic state, then ionized by one additional photon. The resulting distribution of ion vibrational states depends on the properties of the intermediate state and cation ground state. In the simplest case, the intermediate is a Rydberg state—essentially a cation core, loosely coupled to the excited electron. As a consequence of the weak coupling, the molecular geometry is nearly identical to that of the free cation, thus when the Rydberg state is photoionized, the Franck–Condon principle favors leaving the cation in the same vibrational level that was populated in the Rydberg state. By tuning to different vibrational levels of the intermediate state, the ion vibrational level can be tuned, at least in the ideal case. In reality it is necessary to verify state selection by measuring the spectrum of photoelectrons produced in the various REMPI transitions. A number of groups have done the necessary spectroscopy to find REMPI state selection routes for C_2H_2 [22,23], OCS [24], NH_3 [25,26], CH_3CHO [27], C_4H_6 [28], H_2CO [29], and NO_2 [30]. MATI is, in principle, a general method. To date it has been used to rotationally select a number of diatomics [31,32] and to vibrationally select phenol cations [33].

Reactions are measured using a guided-ion-beam tandem mass spectrometer instrument that has been described previously, along with procedures for data acquisition and analysis [20]. Ions are produced in the desired vibrational states by laser ionization schemes appropriate to the molecule in question. Any fragment ions produced in the ionization process are removed by passage through a quadrupole mass filter. In addition, the ion lens set following the quadrupole includes a split center electrode that is used to time-gate the ion pulse, improving the time and translational energy resolution of the experiment. Typically, the resulting state-selected beam has a kinetic energy width of only ∼0.1 eV. The vibrational state-, mass-, and energy-selected ions are then guided into a system of eight-pole radio frequency (rf) ion guides. In the first guide segment, ions pass through a 10 cm long scattering cell, containing the neutral target gas at a pressure low enough to give single-collision conditions ($\sim 10^{-4}$ Torr). Product ions and unreacted primary ions are collected by the ion guide, and passed into a second, longer guide segment for time-of-flight (TOF) analysis, and finally are mass analyzed and counted.

Integral cross-sections are calculated from the ratio of reactant and product ion intensities, and the calibrated target gas pressure × length product. TOF is used to measure the actual reactant ion beam velocity distribution (and thus the E_{col} distribution) at each nominal E_{col}. Two types of differential cross-sections can be measured [20,34–36]. TOF is always used to measure the product ion axial velocity distribution, i.e., the projection of the full velocity distribution on the ion guide axis. Because our experimental geometry

is symmetric about the guide axis, the relative velocity of the reactants and the velocity of the center-of-mass system in the lab frame (V_{CM}) are both co-axial with the ion guide, on average. As a consequence, dynamical information can be gleaned directly from the axial velocity (v_{axial}) distributions. For example, if reaction proceeds via a complex with the lifetime long compared to its rotational period ($\tau_{rotation}$, typically a few picoseconds), the resulting v_{axial} distribution must be symmetric about V_{CM}. Conversely, an asymmetric v_{axial} distribution is a clear sign that the reaction is not mediated by a long-lived complex, and also reveals the predominant scattering mechanisms (i.e., forward or back-scattering). The v_{axial} distributions provide no information about the extent of side-ways scattering, however, thus any quantitative interpretation (e.g., extracting angular or energy distributions) requires either making assumptions about the reaction mechanism, or measurement of the full doubly differential cross-section. The doubly differential cross-section can be recovered from a set of TOF measurements taken with different ion guide rf amplitudes, as described by Gerlich [37,38]. By fitting this set of distributions, we obtain a full differential cross-section, at the same time correcting for experimental broadening from the ion beam and target velocity distributions [34].

To aid interpretation, ab initio calculations were performed at various levels of theory using either GAUSSIAN 98 [39] or GAUSSIAN 03 [40], to map out the energetics of the reaction coordinates (complexes, TSs, ...). For comparison with experiment, the RRKM program of Zhu and Hase [41], was used to calculate statistical lifetimes and decay branching ratios for any complexes on the reaction path. For selected systems, we also carried out ab initio direct dynamics trajectory calculations by using the VENUS program of Hase et al. [42] to set up trajectory initial conditions, and the updating Hessian method of Schlegel and coworkers [43], incorporated into GAUSSIAN [40,44] to propagate trajectories.

3. Dynamical control in complex-mediated ion–molecule reactions

3.1. $H_2CO^+ + CD_4$

The $H_2CO^+ + CD_4$ system [45–47] provides an example of dynamical control of reaction at low E_{col}, even though the reaction is complex-mediated in this energy range. We have performed both experimental and direct dynamics trajectory studies of this system [46,47], and consequently have an unusually detailed picture of the reaction mechanism. Absolute reaction cross-sections and recoil velocity and angular distributions were measured over a wide range of E_{col}, for seven different vibrational states of the reactants, including the ground state, and excited states with pure excitation of five different H_2CO^+ vibrational modes or with thermal excitation of CD_4 deformation vibrations. The following reactions

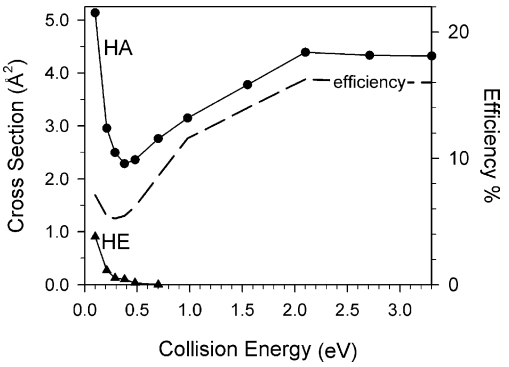

Fig. 1. Cross-sections for the reaction of ground state H_2CO^+ with CD_4. The right axis shows the reaction efficiency.

are observed:

$$H_2CO^+ + CD_4 \rightarrow H_2COD^+ + CD_3$$

(hydrogen abstraction = HA) $\Delta_r H^\circ = -0.18$ eV

$$H_2CO^+ + CD_4 \rightarrow CD_3CHOD^+ + H$$

(hydrogen elimination = HE) $\Delta_r H^\circ = -0.67$ eV

The integral cross-sections for reaction of ground state H_2CO^+ with CD_4 are shown in Fig. 1 over the CM E_{col} range from 0.09 to 3.3 eV. Also plotted, against the right axis, is the reaction efficiency, i.e., the ratio of the total reaction cross-section to the collision cross-section. The collision cross is estimated as the greater of the hard sphere cross-section ($\sigma_{hardsphere}$) and the capture cross-section ($\sigma_{capture}$). Both the individual cross-section and the efficiency plot suggest that there are two mechanistically distinct energy ranges. At low E_{col}, the efficiency is reduced by increasing energy, and is quite low—unusual for a barrierless ion–molecule reaction where the dominant channel is simple atom transfer. Although energetically more favorable, HE accounts for only ~15% of the total reaction cross-section at low E_{col} and is completely suppressed by increasing E_{col}. Given the rearrangements required to generate HE products, this channel almost has to be mediated by a complex. At low E_{col} the dominant HA channel is also strongly inhibited by collision energy. The HA channel approaches a minimum at $E_{col} = 0.4$ eV (where HE disappears entirely), then rebounds, eventually becoming energy-independent at high E_{col}. Clearly a new reaction mechanism is responsible for HA at high E_{col}, and the energy independence observed above ~2 eV suggests that efficiency is controlled by collision geometry, rather than energetic considerations.

The product recoil velocity and angular distributions reinforce the mechanistic picture inferred from the energy dependence of the cross-sections. Velocity distributions were not analyzed for the HE channel, because the kinematics for H elimination preclude extracting useful velocity information. On the other hand, the data for HA provide substantial dynamical insight. Full doubly differential cross-sections were mea-

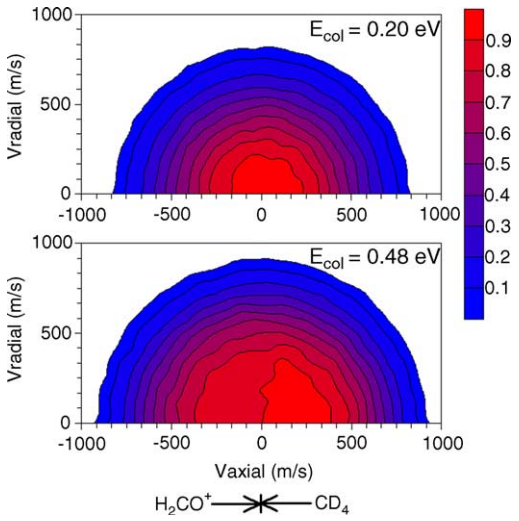

Fig. 2. Center-of-mass velocity maps from fitting the full v_{axial}/v_{radial} distributions for H_2COD^+ produced in reaction of $H_2CO^+ + CD_4$ at $E_{col} = 0.2$ and 0.48 eV.

sured, and are plotted as velocity maps in Fig. 2, for $E_{col} = 0.2$ and 0.48 eV. For $E_{col} = 0.2$ eV, the map is forward–backward symmetric, and the corresponding E_{recoil} distribution is featureless, and peaked at low recoil energies. This is just the behavior expected for decay of a complex that lives long enough to rotate away any asymmetry in angular distribution, and to randomize energy. For $E_{col} = 0.48$ eV, the map is slightly asymmetric, suggesting that the complex lifetime has dropped to about one rotational period (0.8 ps). The distributions become strongly forward peaked at high collision energies, indicating a transition to a direct H-stripping reaction mechanism.

Fig. 3 shows a simplified reaction coordinate diagram for $H_2CO^+ + CH_4$. The energetics are taken from experimental data where available [48], and otherwise from B3LYP/6-311++G** calculations. There are a number of additional TSs and complexes of $C_2H_6O^+$ stoichiometry, not shown because they clearly are not significant in the energy range of interest [46]. Three complexes are important in the reaction. Complex A is a reactant-like complex with H_2CO^+ electrostatically bound to CD_4 with a OC(H)H–CH_4 distance of 2.03 Å, and binding energy with respect to reactants of ~0.4 eV (~four times our lowest collision energy). Complex B is product-like, with H_2COD^+ hydrogen-bonded to planar CD_3 with a hydrogen bond length of 1.70 Å. The binding energy is about the same as in complex A, but in this case, relative to HA products. Finally, there is a covalently bound complex with ethanol structure, bound by ~1 eV relative to reactants.

Complex B can form directly from reactants with no activation barrier, or by isomerization from complex A via TS(A–B) with an energy barrier of 0.16 eV relative to complex A. Accordingly, there are two possible pathways leading to HA products at low collision energies. The direct pathway: reactants → complex B → $H_2COH^+ + CH_3$, presumably can occur for collisions with reactant orientation appropriate for O attack on one of the methyl hydrogen atoms. The indirect route is: reactants → complex A → TS(A–B) → complex B → $H_2COH^+ + CH_3$, where complex A serves as a precursor, allowing HA in collisions with non-optimal reactant orientations. The calculated low energy pathway for HE is reactants → complex A → TS(A–B) → complex B → TS(B–$CH_3CH_2OH^+$) → $CH_3CH_2OH^+$ → CH_3CHO-H^+ → H, where $CH_3CH_2OH^+$ is the most stable of the possible covalent complexes, and can eliminate H via a

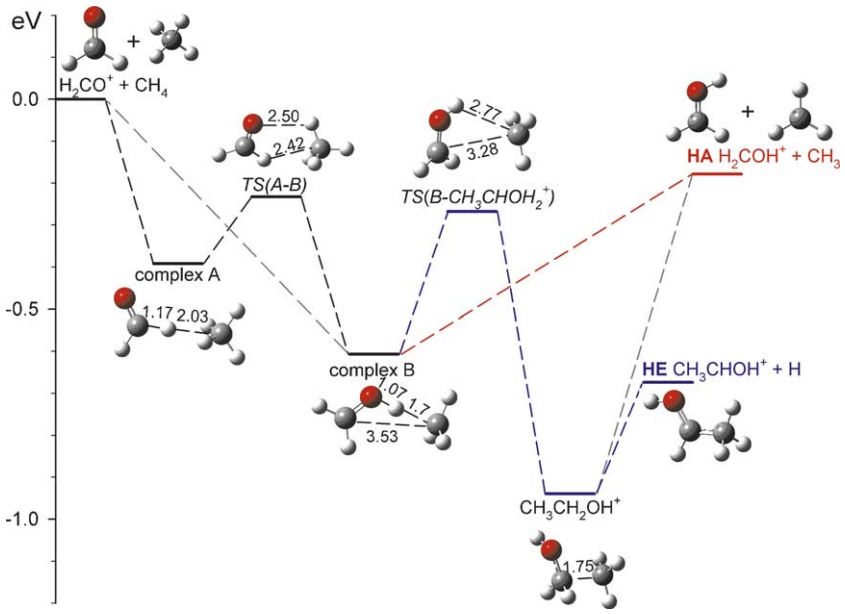

Fig. 3. Schematic reaction coordinate for $H_2CO^+ + CH_4$. Energies are derived from a combination of experimental and B3LYP/6-311++G** values, the latter including zero point energies.

low energy pathway, directly forming the most stable HE product isomer, CH_3CHOH^+.

To test whether these complexes are strongly enough bound to account for the complex-mediated mechanism inferred from the low E_{col} experimental results, two types of calculations were made. RRKM theory was used to estimate the lifetimes and decomposition branching of the complexes as a function of collision energy. The reactant-like complex A is found to have a lifetime ranging from 2.4 ps at $E_{col} = 0.09$ eV to 0.45 ps at $E_{col} = 0.48$ eV. The RRKM lifetime of complex A is consistent with the lifetimes extracted from the experimental differential cross-sections. This complex decays predominantly back to reactants; the isomerization to complex B (and thus to products) varies from 21% at low energies to 10% at $E_{col} = 0.48$ eV. Because complex B can decay to products via a loose, orbiting TS, its lifetime is substantially shorter than that of complex A, suggesting that the experimental collision times mostly originate in complex A. Furthermore, the decay of complex B back to reactants is negligible, therefore, formation of complex B is expected to be the rate-limiting step in the mechanism. In principle, complex B can form directly from reactants or by isomerization from complex A, however, comparison of RRKM and experimental branching ratios suggests that around 90% of complex B formation occurs by isomerization from complex A. We will henceforth refer to complex A as the "precursor complex".

Once formed, complex B decays predominantly to HA products, with 20–30% branching to HE products. The overall branching between HA and HE, and "back to reactants" is calculated to range from 12:6:82 at $E_{col} = 0.09$ eV, to 8:1:91 at $E_{col} = 0.29$ eV. The only significant discrepancy with experiment is that the total reactivity (HA + HE) is calculated to be about two times higher than the experimental reaction efficiency. This discrepancy is not surprising, because the RRKM-based model only gives the branching out of the set of complexes (precursor A, B, and $CH_3CH_2OH^+$), but omits consideration of the complex formation probability. The obvious implication is that about half of low E_{col} collisions simply result in rebound of reactants—not surprising given the weak binding in the precursor complex.

This mechanistic picture was tested by direct dynamics trajectory calculations of the collision dynamics, with forces evaluated at the MP2/6-31G* level of theory. At high collision energies these calculations revealed the reaction mechanism in some detail [47]. For the long collision times at low E_{col}, it is not feasible to follow trajectories to completion, and even partial trajectories take several days of CPU time each. Nonetheless, the trajectories are interesting. At $E_{col} = 0.1$ eV, for example, every trajectory was found to result either in rebound back to reactants, or trapping into a reactant-like complex, i.e., the precursor complex. No trajectories leading directly to the product-like complex B were seen. These results confirm the main conclusion of the RRKM study: trapping into the precursor complex is not 100% efficient. Direct complex B formation is not efficient, ergo the dominant low E_{col} mechanism is reactants → precursor → complex B → products. It was not feasible to run trajectories long enough to estimate the precursor lifetime, however, it is clearly at least in the picosecond range at $E_{col} = 0.1$ eV, consistent with both RRKM and experimental lifetime estimates.

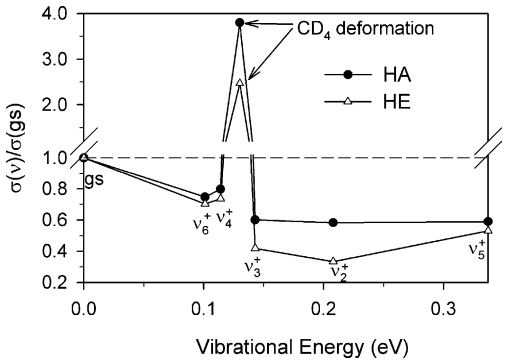

Fig. 4. Vibrational enhancement/inhibition factors vs. E_{vib} for reaction of $H_2CO^+ + CD_4$ averaged at low collision energy range of 0.1–0.2 eV.

For this system, the experimental results, RRKM calculations, and trajectories all indicate that the mechanism is complex-mediated at low E_{col}. Branching ratios, recoil energy distributions, and collision times are all consistent with statistical theory, thus this is a system where dynamical effects might be expected to be small. This expectation is shown to be false by the strong dependence of reactivity on reactant vibrational state. Fig. 4 shows the vibrational effects on both HA and HE channels averaged over the E_{col} range from 0.1 to 0.2 eV, i.e., in the range where the mechanism is clearly complex-mediated. The vibrational effects are given as the ratio $\sigma(v)/\sigma(gs)$ plotted against vibrational energy, where $\sigma(v)$ and $\sigma(gs)$ are the cross-sections for reaction of vibrationally excited, and ground state reactants, respectively. Each point corresponds to a particular reactant state. Points labeled "ν_n^+" correspond to $H_2CO^+(\nu_n^+)$ reacting with ground state CD_4. The points labeled "CD_4 deformation" correspond to reaction of ground state H_2CO^+ with CD_4 where a combination of ν_2 and ν_4 deformation modes have been excited by heating the CD_4 gas to 580 K.

In thermal preparation of vibrationally excited CD_4, the rotational temperature is also increased, and it is conceivable that the enhancement might be entirely or partially from reaction of rotationally excited CD_4. Significant rotational effects are not likely because the thermal increase in both rotational energy and angular momentum are small compared to the energy and angular momentum available from the collision. Nonetheless, this possibility was check by running direct dynamics trajectories for vibrationally excited CD_4 at both $T_{rot} = 300$ and 580 K, with the result that there are no significant effects of T_{rot}, as expected.

Note that the vibrational effects on the HA and HE channels are similar, suggesting that they are controlled by a common rate-limiting step, consistent with the reaction paths outlined above. All H_2CO^+ vibrations inhibit reaction

and the vibrational effects are mode dependent. In contrast CD_4 distortion strongly enhances reaction. It is interesting to compare the effects of vibrational and collision energy in the low E_{col} regime, where the energies are comparable. For example, the ground state total reaction cross-section at $E_{col} = 0.09$ eV is 6.0 Å^2. Addition of 0.1 eV of E_{col} cuts the reactivity in half, whereas excitation of H_2CO^+ ν_4^+ (0.114 eV) at $E_{col} = 0.09$ eV only drops the reactivity by 25%. Addition of roughly the same energy as CD_4 distortion vibration increases reactivity by >300%. Clearly, the idea that energy is randomized at the rate-limiting reaction step, inherent in any purely statistical mechanism, is wrong.

For all H_2CO^+ modes, the inhibition from vibrational excitation is less than from addition of the equivalent amount of collision energy. This general trend (though not the mode-specificity) is expected for the precursor complex-mediated mechanism outlined above. Increasing E_{col} decreases the capture collision cross-section, and adds both energy and angular momentum to the initially formed precursor complex. In a statistical mechanism, additional energy and angular momentum both favor dissociation of the precursor back to reactants (via a high energy orbiting TS), thereby suppressing reaction via the lower energy, but tight TS(A–B). In contrast, vibrational excitation has no effect on the capture cross-section and provides no angular momentum, thus the only factor tending to suppress reaction is the additional vibrational energy.

One of the more surprising observations is that this pattern of vibrational enhancements and inhibitions is preserved up to the highest collision energies studied, even though the reaction mechanism clearly switches to direct stripping. This similarity suggests that reactant vibration affects passage through a critical point on the reaction path, and that this critical point is common to both the complex-mediated and direct reaction mechanisms. This commonality is important, because it means that trajectories calculated at high E_{col}, which are computationally tractable, should provide some insight into the critical point dynamics at low E_{col}.

In summary, a statistical mechanism based on the reaction coordinate in Fig. 3 appears to account for the main features of the ground state reaction at low E_{col}. On the other hand, such a mechanism cannot account for the large enhancement from CD_4 vibration, the mode specificity of the H_2CO^+ vibrational effects, or the fact that the H_2CO^+ vibrational effects are nearly independent of E_{col}. The failure to account for the vibrational effects indicates that the mechanism is incomplete, i.e., that dynamical effects must be included, even at the lowest collision energies.

The first step toward understanding the vibrational dynamics is to identify the point on the reaction coordinate where effects originate. The only way the vibrational effects can be so large (ranging from 4× enhancement to 3× inhibition) and so strongly mode specific, is if vibration influences the limiting step of the reaction mechanism. Furthermore, this limiting step must occur prior to transition to a product-like geometry (in this case, prior to formation of complex B), because the initial vibrational mode would certainly be scrambled after this point. The two candidate limiting steps are formation of the precursor, and isomerization of the precursor to complex B.

There are two limiting cases. If the inter-molecular potential in the precursor is strongly dependent on the vibrational coordinates of the individual molecules, then reactant vibration could influence precursor formation, however, the initial vibrational modes would scramble upon precursor formation. At the other extreme, vibration should have little effect on precursor formation if the inter-reactant potential is weak and weakly coupled to vibration of the individual reactants. At the same time, however, vibrational modes in such a complex would scramble slowly, allow the possibility of influencing the subsequent transition to products.

For this reaction, the experiments suggest that the latter possibility (weak coupling of vibration in the precursor complex) is correct. This can be seen by examining the dependence of the recoil angular distributions on E_{col} and reactant vibrational state. For ground state H_2CO^+, the transition from forward–backward symmetric to forward-peaked distributions first becomes noticeable at $E_{col} \approx 0.5$ eV, and the fitted $\tau_{collision}$ at that energy is ~0.6 ps. This result is in excellent agreement with the RRKM lifetime calculated for the precursor complex, which drops to about half a picosecond at $E_{col} \approx 0.5$ eV. If reactant vibration were coupled strongly in the precursor complex, then the available energy would increase significantly, and asymmetric angular distributions would appear at lower E_{col}. Taking the H_2CO^+ ν_5^+ mode (0.337 eV) for example, the RRKM precursor lifetime would drop to 0.42 ps at $E_{col} = 0.09$ eV, compared to 2.4 ps for the ground state at this energy. With such a large decrease in precursor lifetime, the transition to asymmetric distributions would already be apparent at the lowest E_{col}. In fact, the transition is found to be independent of reactant vibrational state, indicating that the vibrational energy is not available to drive decay of the precursor. The only noticeable vibrational effect on the recoil behavior is that the recoil energy distributions broaden slightly, implying that reactant vibration does couple at some point in the reaction coordinate, so that the vibrational energy is ultimately available to the products.

The trajectory results are consistent with this conclusion, and provide interesting insight into just how weakly coupled such complexes can be. For a weakly bound complex formed with energy above its dissociation limit, one expects the structure to be floppy, with large amplitude excursions from the equilibrium geometry. At least for this system, however, the trajectories reveal that "floppy" considerably understates the situation. In a typical complex-forming trajectory at $E_{col} = 0.1$ eV, the reactants have an initial "collision", converting energy in relative translation mostly to rotational motion of the H_2CO^+ and CD_4 moieties. At the relatively large intra-moiety separation in the precursor, the potential anisotropy is weak, so that the complex is essentially freely rotating H_2CO^+ and CD_4 moieties that occasionally "collide"

with each other. For this system, the precursor complex exerts no control over reactant orientation, and merely provides the reactants with repeated opportunities to "collide", thereby increasing the chances that they will find the correct geometry. The coupling between the separation coordinate and the internal rotations of H_2CO^+ and CD_4 is so weak that we never observed breakup of such a complex, even in a few trajectories allowed to run for 7 ps—substantially greater than the RRKM-estimated lifetime. Weak coupling of relative motion with H_2CO^+ and CD_4 vibration is also not surprising for low E_{col}, where the time scale of vibration is poorly matched to relative translation.

The remaining question is how reactant vibration actually enhances or inhibits the H-abstraction event. At least for high E_{col}, where direct dynamics trajectories are feasible, we were able to show quantitatively how methane vibrational enhancement originates, which is probably the first time the origin of a polyatomic vibrational effect has been unraveled in detail. According to the trajectory results at E_{col} = 1.7 eV, the reaction is very orientation sensitive, occurring only when CD_4 approaches with one of the D atoms in the H_2CO^+ plane, and with the D–O–C angle in the range between 90° and 120°, i.e., close to the DOC bond angle in the H_2COD^+ product. Such a narrow range of reactive orientations is consistent with the low reaction efficiency. One possibility for the origin of the vibrational effects would be if CD_4 distortion relaxed the orientation sensitivity.

The trajectories show that this is not the case. Instead, the CD_4 vibration enhances reactivity only for favorable orientations, and there appear to be two effects contributing to this enhancement. Vibrationally excited CD_4 has a significantly higher probability of colliding while distorted into a product-like geometry (i.e., near planar CD_3 in H_2CO–D–CD_3), and the reaction probability was found to be near unity for such collisions. In addition, vibrationally excited CD_4 is more reactive than ground state CD_4, even for collisions where the CD_4 is near its equilibrium geometry. In these collisions the vibrational enhancement comes from the vibrationally induced velocities of the D atoms, which tend to carry the system toward a product-like geometry. Both vibrational distortion and vibrational velocity effects are important, and roughly equally contribute to this system at E_{col} = 1.7 eV. At this energy, it turns out that the CD_4 vibrational period is comparable to the time when the colliding reactants are interacting strongly, and this probably accounts for the similar contributions of distortion and velocity effects.

Another way of looking at the CD_4 vibrational effects is in terms of "Polanyi rules", which correlated the relative efficacy of vibrational and collision energy in driving reactions over a barrier, with the position of the barrier on the potential energy surface for a model A + BC reaction [49]. For reactions with early (i.e., reactant-like) barriers, collision energy is predicted to be effective, and E_{vib} is ineffective, at driving reaction. Conversely, for late (product-like) barriers, E_{vib} is predicted to be more effective. The rate-limiting TS for $H_2CO^+ + CD_4$ reaction is quite reactant-like (TS(A–B),

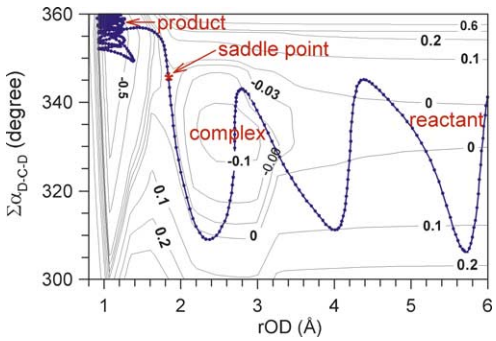

Fig. 5. Potential energy contour map for $H_2CO^+ + CD_4$ calculated at MP2/6-31G*. The numbers are the potential energy (eV) relative to the reactant. The dotted line is a reaction trajectory at E_{col} = 1.7 eV.

Fig. 3). On the other hand, trajectory results indicate that the actual hydrogen abstraction event does happen late in the collision. It is unclear, therefore, how one might rationalize the large enhancement from CD_4 vibration according to "Polanyi rules". In Fig. 5, we show a two-dimensional cut through the 21-dimensional potential surface [47], constructed to show the typical reaction path taken by vibrationally excited reactants. The dimensionality was reduced by fixing the relative orientation of CD_4 and H_2CO^+ so that CD_4 approaches in the H_2CO^+ plane, with the DOC angle fixed at 110°, and one D atom pointing at the O atom. This simply amounts to focusing attention on the most reactive orientation. We further reduced dimensionality by forcing the spectator CD_3 moiety to remain in C_{3V} symmetry. In the plot, one axis is rOD, i.e., the distance between the O atom and the D atom being abstracted, i.e., the reactant approach coordinate. The other coordinate is designed to be a measure of both CD_4 reactant distortion, and of the transition to products. The coordinate is the sum of the three DCD angles in the spectator CD_3. The reactant CD_4 equilibrium geometry corresponds to $\sum\alpha_{D-C-D} = 328°$, and the planar CD_3 product corresponds to $\sum\alpha_{D-C-D} = 360°$. On this reduced surface, there is a saddle point that corresponds to a "late" barrier in the context of the Polanyi rules. Note that this saddle point is product-like in terms of CD_4 distortion, however, it is still quite reactant like with respect to bond lengths (i.e., rCD = 1.1 Å, and rOD = 1.8 Å). A typical reactive trajectory is projected onto the reduced surface. As expected, the trajectory does not follow the minimum energy path due to the kinetic energy in vibration and E_{col}. Instead, that the methane vibrational motion gives the system substantial momentum transverse to the entrance valley, and this momentum carries the system across the saddle point. The take-home lesson here is that while it may be quite difficult to understand the nature of the motion on a high dimensionality surface, in a sense the vibrational effect still result from behavior reminiscent of much simpler systems.

Understanding the H_2CO^+ vibrational effects is more difficult. Unlike the methane moiety, which undergoes geometry distortion during the reaction, none of the H_2CO^+ vibrational modes is obviously coupled to the reaction coordinate. A

theoretical effort to unravel the complex dynamics of these modes is underway.

3.2. $C_2H_2^+ + CH_4$

The reaction of $C_2H_2^+$ with CH_4 has been the subject of a number of experimental and theoretical studies [20,50–59], and our group probed the effects of collision energy and $C_2H_2^+$ vibrational excitation on this reaction [20,55,56]. This system shows very large and mode-specific vibrational effects, despite clearly being mediated by one or more intermediate complexes. In our original study of this system, we speculated about the existence of weakly bound and covalently bound complexes. Subsequently Kippenstein [60] and Cui et al. [61] calculated the structures of several intermediates at the MP2/6-31G* and B3PW91/6-311G** levels of theory. For the present study, we recalculated the stationary points for this system at B3PW91/6-31+G**, B3LYP/6-31+G**, MP2/6-31+G** and G3 levels of theory. The results are in reasonable agreement with the previous calculations, and the G3 results are in best agreement with experiment. A schematic reaction coordinate for the $C_2H_2^+ + CH_4$ reaction is mapped out in Fig. 6. The energetics are derived from a combination of experimental [48,62] and G3 (298 K) values.

The reaction of $C_2H_2^+$ with CH_4 has the following channels observed at low E_{col}:

$$C_2H_2^+ + CH_4 \rightarrow C_2H_3^+\,(\text{bridged}) + CH_3 \quad (\text{HA})$$
$$\Delta_r H^\circ = 0.05\,\text{eV}$$

$$C_2H_2^+ + CH_4 \rightarrow C_2H_3^+\,(\text{classical}) + CH_3 \quad (\text{HA})$$
$$\Delta_r H^\circ = 0.23\,\text{eV}$$

$$C_2H_2^+ + CH_4 \rightarrow C_3H_4^+ + H_2 \quad (H_2\text{-elimination})$$
$$\Delta_r H^\circ = -1.32\,\text{eV}$$

$$C_2H_2^+ + CH_4 \rightarrow C_3H_5^+ + H \quad (\text{H-elimination} = \text{HE})$$
$$\Delta_r H^\circ = -0.93\,\text{eV}$$

Note that there are two forms of $C_2H_3^+$ as shown in Fig. 6, the bridged form being more stable. The main points of the computational study are as follows: (1) both weakly bound and covalently bound complexes are available to mediate reaction. We will refer to the weakly bound species collectively as "the precursor complex". Note that the precursor in this system is more strongly bound, with a less reactant-like geometry than in the $H_2CD^+ + CD_4$ system discussed above. (2) At the G3 level of theory, only a classical form of the precursor complex ("classical complex") is stable, however, if the geometries are optimized at the MP2/6-31+G** level, there is also a precursor complex with bridged geometry (inset to Fig. 6). Given the small energy differences and barrier separating these isomers, the precursor is probably best considered as a single floppy complex with one or more shallow

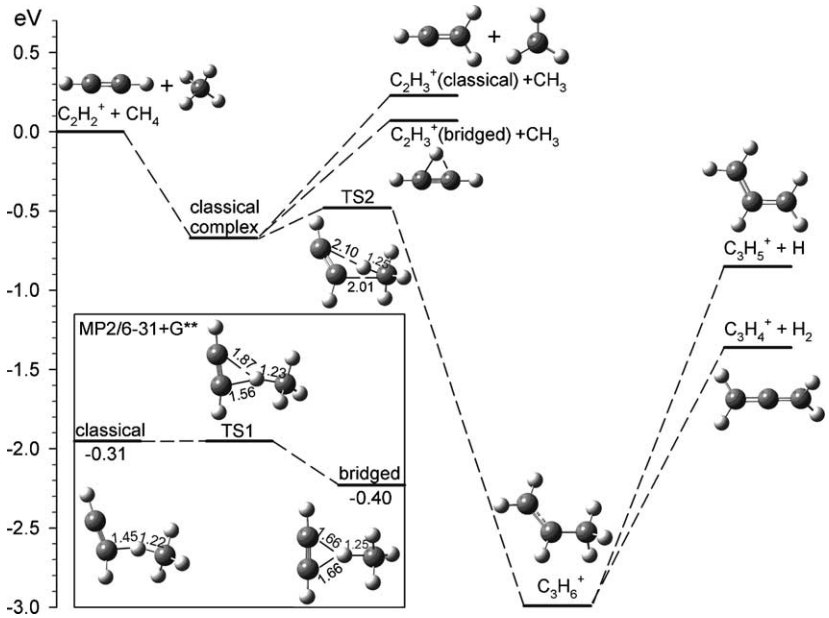

Fig. 6. Schematic reaction coordinate for $C_2H_2^+ + CH_4$. Energies are derived from a combination of experimental and G3 (298 K) values. The insert shows the interconversion between "classical" and "bridged" complex, calculated at MP2/6-31+G**.

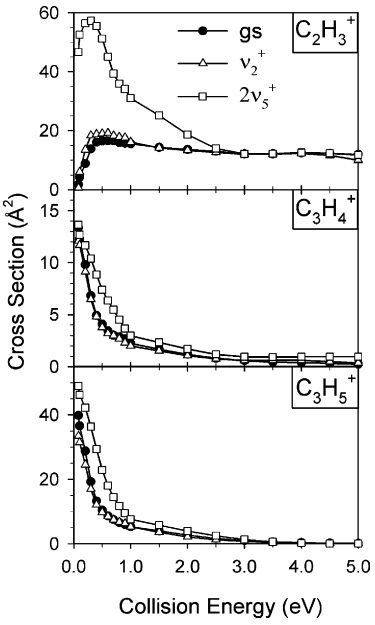

Fig. 7. Reaction cross-sections for the ground state and vibrational excited $C_2H_2^+$ with CH_4.

local minima. No barrier separates the precursor complex from reactants or from the HA product channels. (3) There are a number of covalently bound, linear and cyclic $C_3H_6^+$ isomers, only the most stable of which is shown. These strongly bound complexes will collectively be referred to as "covalent $C_3H_6^+$". (4) The precursor complex can isomerize to covalent $C_3H_6^+$ via TS2.

The integral cross-sections for the three product channels are shown in Fig. 7 as a function of E_{col}, for three different vibrational states of $C_2H_2^+$, including the ν_2^+ (C–C stretch, 0.225 eV), $2\nu_5^+$ (overtone of the *cis*-bend, 0.155 eV), as well as the ground state. The dominant channels at low collision energies are $C_3H_5^+ + H$ and $C_3H_4^+ + H_2$. These two products require formation of C–C bonds and H atom migration along the carbon backbone, and therefore must form via H- or H_2-elimination from covalent $C_3H_6^+$. We also examined the isotope distribution in reaction of $C_2H_2^+$ with CD_4, and for the H- and H_2-elimination channels at all E_{col}, the distribution of deuterium labels is approximately that expected from combinatorial statistics. The RRKM lifetime for the most stable isomer of covalent $C_3H_6^+$ varies from approximately 10 ns at our lowest collision energies to 70 ps at 3.0 eV—apparently long enough for isotope scrambling.

Both these channels are inhibited by collision energy, very weakly inhibited by ν_2^+, but significantly enhanced by $2\nu_5^+$ excitation. The smaller inhibition by ν_2^+, relative to that from an equivalent increase in E_{col}, can be rationalized in a statistical picture. As discussed above, increasing E_{col} decreases the capture cross-section and increases the angular momentum—both factors that tend to suppress reaction. On the other hand, the large enhancement from $2\nu_5^+$ excitation is clearly not consistent with a purely statistical mechanism.

The similar collision energy and vibrational state dependence for the two $C_3H_x^+$ channels suggests that they share a common rate-limiting step, where the collision energy and vibrational dependence is determined. As discussed above, this rate-limiting step must be early enough on the reaction coordinate, so that the reactant vibrational mode is not yet scrambled. Once past this limiting step, the branching between H- and H_2-elimination appears to be statistical, with the lower energy H_2-elimination channel inhibited by a relatively tight TS for H_2-elimination. As in the $H_2CO^+ + CD_4$ example above, it is clear that mode scrambling must accompany the transition to the covalent complex, therefore, vibrational excitation must be controlling either formation of the precursor, or the transition from precursor to covalent structures. In the $H_2CO^+ + CD_4$ system, the precursor is bound by only 0.4 eV, and the structure is quite reactant-like. Here the precursor binding energy is about doubled, and there is substantial distortion of both moieties from the reactant geometries. As a consequence, it is not clear if the $C_2H_2^+$ vibrations could be coupled weakly enough to survive in the precursor for a time on the order of its lifetime.

In addition to these two exoergic channels, there is a substantial cross-section for the hydrogen abstraction (HA) channel as soon as the available energy is sufficient to overcome the endoergicity. The HA reaction is strongly enhanced by E_{col} near threshold, then nearly E_{col}-independent above 0.5 eV. Excitation of the C–C stretch (ν_2^+) slightly increases the magnitude of the HA cross-section, but surprisingly, has no effect on the threshold energy, within experimental error. The implication is that this mode is essentially uncoupled to the reaction coordinate, such that its energy is unavailable to drive reaction. In contrast, *cis*-bend ($2\nu_5^+$) excitation results in a large increase in HA cross-section, and shifts the energy dependence so that we are no longer able to resolve the threshold.

A complication in thinking about the HA channel is that these products can form by direct H abstraction, by precursor-mediated H transfer, and by CH_3 elimination from covalent $C_3H_6^+$. In order to estimate the extent to which CH_3 elimination from covalent $C_3H_6^+$ contributes to $C_2H_3^+$, we measured the isotope distribution produced in reaction of $C_2H_2^+$ with CD_4. As noted, the $C_3H_x^+$ channels, which clearly are mediated by covalent $C_3H_6^+$, have essentially combinatorial D-label distributions. It turns out that only 10–15% (depending on E_{col}) of the HA product is $C_2HD_2^+$, compared to ~60% that would be expected from combinatorial statistics. This demonstrates that CH_3 elimination from covalent $C_3H_6^+$ is a relatively minor contribution to the HA channel.

The other issue is whether a complex is required at all, or if HA might be occurring by a direct mechanism. Here we turn to measurements of the product recoil angular distributions, shown in Fig. 8. The top three distributions in Fig. 8 illustrate the v_{axial} distribution for $C_2H_2D^+$ products formed in reaction of $C_2H_2^+$ with CD_4, i.e., HA without H/D exchange. For the lowest E_{col} (=0.25 eV), the distribution is forward–backward symmetric, within experimental error. The symmetric distri-

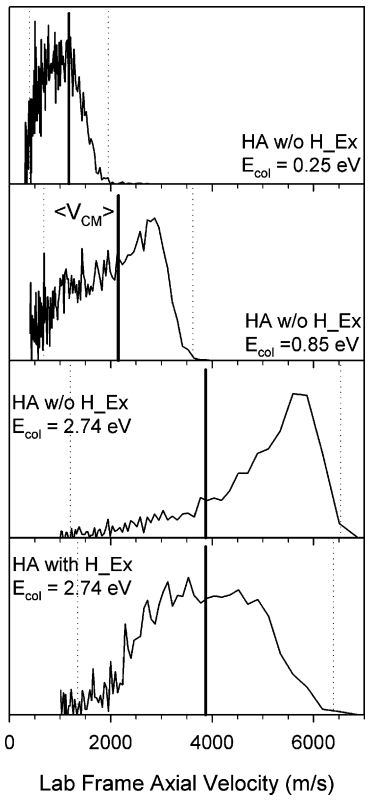

Fig. 8. Axial recoil velocity distributions for $C_2H_2D^+$ and $C_2HD_2^+$ (bottom frame) produced in reaction of $C_2H_2^+ + CD_4$. Heavy vertical lines: $\langle V_{CM}\rangle$. Dotted vertical lines: the limit of velocities allowed by conservation of energy.

bution remains up to $E_{col} = 0.5$ eV. As explained above, such a symmetric distribution is consistent with a mechanism mediated by a complex that lives more than a rotational period. The collision times extracted from fitting these distributions for $E_{col} \leq 0.5$ eV are consistent with RRKM estimates of the lifetime for the precursor complex. For example, the RRKM precursor lifetime is 1.8 ps at $E_{col} = 0.4$ eV. For comparison, this is an order of magnitude longer than the direct collision time, estimated here is the time it would take reactants to move 5 Å relative to each other at the collision velocity. Therefore, the precursor lifetime is mechanistically significant, and consistent with statistical decay. At the intermediate E_{col} of 0.84 eV, the distribution is becoming asymmetric, indicating that the collision time is dropping below the complex rotational period. At the highest E_{col} of 2.74 eV, the distribution is peaked well forward of $\langle V_{CM}\rangle$, which is a characteristic of a direct reaction.

The bottom frame in Fig. 8 shows the v_{axial} distribution at $E_{col} = 2.74$ eV for the $C_2HD_2^+$ product, i.e., for HA products with H/D exchange, presumed to result mostly by methyl elimination from covalent $C_3H_6^+$. This channel remains forward–backward symmetric at all energies, consistent with the long RRKM lifetime calculated for the covalent complex (70 ps at this energy). Further evidence that HA with H/D exchange is mechanistically distinct from HA without H/D exchange, comes from the recoil energy distribution. Only about 10% of E_{avail} is found to appear in E_{recoil} for HA with H/D exchange, compared with 60% for HA without H/D exchange. The conclusion is that ~15–20% (depending on collision energy) of the HA products form by statistical decay of covalent $C_3H_6^+$ intermediates. The balance of HA products form by decay of the precursor complex at low E_{col}, and by direct HA at high E_{col}.

In summary, we have two basic reaction channels at low E_{col}, both initiated by formation of a precursor complex. The exoergic $C_3H_x^+$ products form when the precursor isomerizes to covalent $C_3H_6^+$, which then decays to a statistical mix of $C_3H_5^+$ and $C_3H_4^+$. At energies above the endoergicity, covalent $C_3H_6^+$ also contributes to the $C_2H_3^+$ channel, but this is neither a major decay channel for $C_3H_6^+$, nor a major contribution to the $C_2H_3^+$ signal. Instead, most $C_2H_3^+$ forms at low E_{col} by H transfer within the precursor complex, which then dissociates to products. Both mechanisms are strongly affected by $C_2H_2^+$ vibration in a mode-specific manner, indicating that this seemingly statistical system is, in fact, strongly influenced by the type of motion imposed on the reactants. For both types of channels, C–C stretch excitation has effects qualitatively similar to, but weaker than those of collision energy, while *cis*-bending vibration causes much larger effects, opposite in sign in the case of the $C_3H_x^+$ channels.

Klippenstein proposed a mechanism to rationalize the vibrational effects within a transition state theory framework [60]. The idea is that the vibrational effects result from competition in breakup of the precursor complex, and that reactant vibration simply provides available energy. The competition is between isomerization to covalent $C_3H_6^+$ (leading to $C_3H_x^+$ products), dissociation to HA products, and dissociation back to reactants. Obviously, a purely statistical model cannot account for the observed highly mode specific behavior. Klippenstein proposed that the mode specificity might be qualitatively rationalized, if different reactant vibrational modes were assumed to couple differently in the precursor. He argued that the C–C stretching vibration is adiabatic in the precursor complex, i.e., so weakly coupled that its energy is not available to drive complex decay, thus accounting for the small effects observed. The bending vibration, on the other hand, was argued to be strongly coupled so that its energy contributes to the energy driving decay of the precursor complex. This assumption leads to the correct prediction that bending excitation should enhance the endoergic HA reaction, although it cannot account for the large magnitude of the enhancement observed. As expected for a model considering only the energy content of the vibrations, bending was also predicted to inhibit the $C_3H_4^+$ and $C_3H_5^+$ channels, whereas they are actually enhanced substantially.

It appears therefore, that even allowing different vibrations to couple differently (i.e., implicitly allowing some dynamical effects), a statistical picture which considers only the *energy* contained in the vibrations, is inadequate to account for the observations. It is also essential to take into account

the *nature* of the vibrational motion, i.e., include dynamics explicitly. In this case, the obvious point is that both reaction channels involve bending and rehybridizing one or both carbon centers on the acetylene reactant. Bending vibration is exactly the type of motion needed to carry the system toward products, whereas C–C stretching vibration is uncoupled to this reaction coordinate. The methane distortion effects in the $H_2CO^+ + CD_4$ system can also qualitatively be rationalized in this manner, because the product CD_3 moiety is planar. On the other hand, we have seen many examples where a simple "distortion toward product geometry" picture does not correctly predict the observed vibrational effects, or where it is not clear how to apply such a picture. The H_2CO^+ vibrations in $H_2CO^+ + CD_4$ are an example of the latter case—they are not obviously coupled to the reaction coordinate, but have large, mode specific effects.

4. Conclusions

Two examples were presented of ion–molecule reactions mediated by long-lived complexes at low collision energies. In both cases, the product branching, E_{col} dependence, and recoil velocity and angular distributions are consistent with statistical complex decay. Measurement of the effects of reactant vibrational excitation shows, however, that the reactivity and product branching are, in fact, controlled by the early time dynamics. These are not isolated examples. Similar effects have been observed for other ion–molecule systems ranging in size from six atoms (e.g., $OCS^+ + OCS$ [63]) to much larger systems such as reaction of $C_6H_5OH^+$ with NH_3 [64] or of acetaldehyde with a number of small molecules [65–68]. As in the examples presented, strong dynamical effects are observed even in reactions that are exoergic, with no activation barriers in excess of the reactant energy.

Dynamical control might seem inconsistent with the assumptions inherent in statistical mechanisms, however, there is no reason that a mechanism cannot combine dynamical control of the early stages of reaction, with statistical effects controlling the late stages, after energy has been randomized. Indeed, many of the systems we have examined with reactant state selection appear to behave just this way, and most of those reactions, precursor complexes appear to play a role in the chemistry. Given that most ion–molecule systems have electrostatically bound, reactant-like complexes available to act as precursors along the reaction path, we infer that many apparently statistical reactions are, in fact, influenced by dynamics.

Of course, dynamical effects will tend to be strongest in reactions where there is a bottleneck that reduces reactivity below the collision limit, however, there are also systems where substantial mode specificity is observed even though the ground state reaction proceeds at the collision limit. For example, in reaction of $C_2H_2^+$ with ND_3 [69], the C–C stretch and $2\nu_{bend}$ excitations have substantial and different effects on reactivity and product branching for $E_{col} < \sim 0.5$ eV, even though the ground state cross-section is at the collision limit. On the other hand, facile reactions such as exoergic proton transfer, are unlikely to depend significantly on reactant vibration. For example, proton transfer between $H_2CO^+ + D_2O$ occurs at the collision limit, regardless of initial state [70].

Acknowledgments

We would like to thank Bill Hase for many helpful discussions over the years. His work on both dynamical and statistical effects on reactivity was instrumental in guiding our thinking about these reactions. This work was supported by the National Science Foundation under Grant No. CHE-0110318.

References

[1] T. Baer, W.L. Hase, Unimolecular Reaction Dynamics: Theory and Experiments, Oxford University Press, New York, 1996.
[2] W.L. Hase, Acc. Chem. Res. 31 (1998) 659.
[3] J.I. Steinfeld, J.S. Francisco, W.L. Hase, Chemical Kinetics and Dynamics, Prentice-Hall International Inc., 1989.
[4] K. Fukui, J. Phys. Chem. 74 (1970) 461.
[5] R.A. Marcus, J. Chem. Phys. 20 (1952) 359.
[6] R.A. Marcus, O.K. Rice, J. Phys. Colloid Chem. 55 (1951) 894.
[7] H.W. Schranz, T.D. Sewell, Theochemistry 368 (1996) 125.
[8] L. Sun, K. Song, W.L. Hase, Science 296 (2002) 875.
[9] S.C. Ammal, H. Yamataka, M. Aida, M. Dupuis, Science 299 (2003) 1555.
[10] J.F. Meagher, K.J. Chao, J.R. Barker, B.S. Rabinovltch, J. Phys. Chem. 78 (1974) 2535.
[11] T. Baer, A.R. Potts, J. Phys. Chem. A 104 (2000) 9397.
[12] P.K. Chowdhury, Chem. Phys. 260 (2000) 151.
[13] L. Oudejans, R.E. Miller, Ann. Rev. Phys. Chem. 52 (2001) 607.
[14] D.S. Tonner, T.B. McMahon, J. Am. Chem. Soc. 122 (2000) 8783.
[15] J. Liu, W. Chen, M. Hochlaf, X. Qian, C. Chang, C.Y. Ng, J. Chem. Phys. 118 (2003) 149.
[16] R.R. Smith, D.R. Killelea, D.F. DelSesto, A.L. Utz, Science 304 (2004) 992.
[17] S.L. Anderson, NATO ASI Ser. C 347 (1991) 183.
[18] S.L. Anderson, Adv. Chem. Phys. 82 (1992) 177.
[19] S.L. Anderson, Acc. Chem. Res. 30 (1997) 28.
[20] Y.-H. Chiu, H. Fu, J.-T. Huang, S.L. Anderson, J. Chem. Phys. 102 (1995) 1199.
[21] L. Zhu, P. Johnson, J. Chem. Phys. 94 (1991) 5769.
[22] M.N.R. Ashfold, B. Tutcher, B. Yang, Z.-K. Jin, S.L. Anderson, J. Chem. Phys. 87 (1987) 5105.
[23] T.M. Orlando, S.L. Anderson, J.R. Appling, M.G. White, J. Chem. Phys. 87 (1987) 852.
[24] B. Yang, M.H. Eslami, S.L. Anderson, J. Chem. Phys. 89 (1988) 5527.
[25] W.E. Conaway, R.J.S. Morrison, R.N. Zare, Chem. Phys. Lett. 113 (1985) 429.
[26] R.D. Guettler, G.C. Jones Jr., L.A. Posey, R.N. Zare, Science 266 (1994) 259.
[27] H.-T. Kim, S.L. Anderson, J. Chem. Phys. 114 (2001) 3018.
[28] J. Liu, S.L. Anderson, J. Chem. Phys. 114 (2001) 6618.
[29] J. Liu, H.-T. Kim, S.L. Anderson, J. Chem. Phys. 114 (2001) 9797.
[30] P. Bell, F. Aguirre, E.R. Grant, S.T. Pratt, J. Phys. Chem. A 108 (2004) 9645.

[31] S.R. Mackenzie, E.J. Halse, F. Merkt, T.P. Softley, Proc. SPIE-Int. Soc. Opt. Eng. 2548 (1995) 293.
[32] R.J. Green, H.-T. Kim, J. Qian, S.L. Anderson, J. Chem. Phys. 113 (2000) 3002.
[33] H.-T. Kim, R.J. Green, J. Qian, S.L. Anderson, J. Chem. Phys. 112 (2000) 5717.
[34] Y.-H. Chiu, H. Fu, J.-T. Huang, S.L. Anderson, J. Chem. Phys. 105 (1996) 3089.
[35] Y.-H. Chiu, PhD Thesis, State University of New York, Stony Brook, 1996.
[36] J. Liu, B. Van Devener, S.L. Anderson, J. Chem. Phys. 116 (2002) 5530.
[37] D. Gerlich, Adv. Chem. Phys. 82 (1992) 1.
[38] S. Mark, D. Gerlich, Chem. Phys. 209 (1996) 235.
[39] M.J. Frisch, G.W. Tucks, H.B. Schlegel, G.E. Scuseria, M.A. Robb, J.R. Cheeseman, V.G. Zakrzewski, J.A. Montgometry, R.E. Stratmann, J.C. Burant, S. Dapprich, J.M. Millam, A.D. Daniels, K.N. Kudin, M.C. Strain, O. Farkas, J. Tomasi, V. Barone, M. Cossi, R. Cammi, B. Mennucci, C. Pomelli, C. Adamo, S. Clifford, J. Ochterski, G.A. Peterson, P.Y. Ayala, Q. Cui, K. Morokuma, D.K. Malick, A.D. Rabuck, K. Raghavachari, J.B. Foresman, J. Cioslowski, J.V. Ortiz, B.B. Stefanov, G. Liu, A. Liashenko, P. Piskorz, I. Komaromi, R. Gomperts, R.L. Martin, D.J. Fox, T. Keith, M.A. Al-Laham, C.Y. Peng, A. Nanayakkara, C. Gonzalez, M. Challacombe, P.M.W. Gill, B.G. Johnson, W. Chen, M.W. Wong, J.L. Andres, M. Head-Gordon, E.S. Replogle, J.A. Pople, GAUSSIAN 98', Gaussian Inc., Pittsburgh, PA, 1998.
[40] M.J. Frisch, G.W. Trucks, H.B. Schlegel, G.E. Scuseria, M.A. Robb, J.R. Cheeseman, J.J.A. Montgomery, T. Vreven, K.N. Kudin, J.C. Burant, J.M. Millam, S.S. Iyengar, J. Tomasi, V. Barone, B. Mennucci, M. Cossi, G. Scalmani, N. Rega, G.A. Petersson, H. Nakatsuji, M. Hada, M. Ehara, K. Toyota, R. Fukuda, J. Hasegawa, M. Ishida, T. Nakajima, Y. Honda, O. Kitao, H. Nakai, M. Klene, X. Li, J.E. Knox, H.P. Hratchian, J.B. Cross, C. Adamo, J. Jaramillo, R. Gomperts, R.E. Stratmann, O. Yazyev, A.J. Austin, R. Cammi, C. Pomelli, J.W. Ochterski, P.Y. Ayala, K. Morokuma, G.A. Voth, P. Salvador, J.J. Dannenberg, V.G. Zakrzewski, S. Dapprich, A.D. Daniels, M.C. Strain, O. Farkas, D.K. Malick, A.D. Rabuck, K. Raghavachari, J.B. Foresman, J.V. Ortiz, Q. Cui, A.G. Baboul, S. Clifford, J. Cioslowski, B.B. Stefanov, G. Liu, A. Liashenko, P. Piskorz, I. Komaromi, R.L. Martin, D.J. Fox, T. Keith, M.A. Al-Laham, C.Y. Peng, A. Nanayakkara, M. Challacombe, P.M.W. Gill, B. Johnson, W. Chen, M.W. Wong, C. Gonzalez, J.A. Pople, Gaussian 03, Revision B.02, Gaussian Inc., Pittsburgh, PA, 2003.
[41] L. Zhu, W.L. Hase, A General RRKM Program (QCPE 644), Quantum Chemistry Program Exchange, Chemistry Department, University of Indiana, Bloomington, 1993.
[42] W.L. Hase, K. Bolton, P. de Sainte Claire, R.J. Duchovic, X. Hu, A. Komornicki, G. Li, K. Lim, D. Lu, G.H. Peslherbe, K. Song, K.N. Swamy, S.R. Vande Linde, A. Varandas, H. Wang, R.J. Wolf, VENUS99: A general chemical dynamics computer program, 1999.
[43] V. Bakken, J.M. Millam, H.B. Schlegel, J. Chem. Phys. 111 (1999) 8773.
[44] M.J. Frisch, G.W. Trucks, H.B. Schlegel, G.E. Scuseria, M.A. Robb, J.R. Cheeseman, V.G. Zakrzewski, J.J.A. Montgomery, K.N. Kudin, J.C. Burant, J.M. Millam, R.E. Stratmann, J. Tomasi, V. Barone, B. Mennucci, M. Cossi, G. Scalmani, N. Rega, S. Iyengar, G.A. Petersson, M. Ehara, K. Toyota, H. Nakatsuji, C. Adamo, J. Jaramillo, R. Cammi, C. Pomelli, J. Ochterski, P.Y. Ayala, K. Morokuma, P. Salvador, J.J. Dannenberg, S. Dapprich, A.D. Daniels, M.C. Strain, O. Farkas, D.K. Malick, A.D. Rabuck, K. Raghavachari, J.B. Foresman, J.V. Ortiz, Q. Cui, A.G. Baboul, S. Clifford, J. Cioslowski, B.B. Stefanov, G. Liu, A. Liashenko, P. Piskorz, I. Komaromi, R. Gomperts, R.L. Martin, D.J. Fox, T. Keith, M.A. Al-Laham, C.Y. Peng, A. Nanayakkara, M. Challacombe, P.M.W. Gill, B. Johnson, W. Chen, M.W. Wong, J.L. Andres, C. Gonzalez, M. Head-Gordon, E.S. Replogle, J.A. Pople, Gaussian 01, Development Version (Revision B.01), Gaussian Inc., Pittsburgh, PA, 2001.
[45] N.G. Adams, D. Smith, D. Grief, Int. J. Mass Spectrom. Ion Phys. 26 (1978) 405.
[46] J. Liu, B.V. Devener, S.L. Anderson, J. Chem. Phys. 119 (2003) 200.
[47] J. Liu, K. Song, W.L. Hase, S.L. Anderson, J. Am. Chem. Soc. 126 (2004) 8602.
[48] S.G. Lias, J.E. Bartmess, J.F. Liebman, J.L. Holmes, R.D. Levin, W.G. Mallard, J. Phys. Chem. Ref. Data 17 (Suppl. 1) (1988) 1.
[49] J.C. Polanyi, W.H. Wong, J. Chem. Phys. 51 (1969) 1439.
[50] J.J. Myher, A.G. Harrison, Can. J. Chem. 46 (1968) 1755.
[51] A.A. Herod, A.G. Harrison, Int. J. Mass Spectrom. Ion Phys. 4 (1970) 415.
[52] N.G. Adams, D. Smith, Chem. Phys. Lett. 47 (1977) 383.
[53] J.K. Kim, V.G. Anicich, J.W.T. Huntress, J. Phys. Chem. 81 (1977) 1798.
[54] K. Honma, I. Tanaka, J. Chem. Phys. 70 (1979) 1893.
[55] T.M. Orlando, B. Yang, S.L. Anderson, J. Chem. Phys. 90 (1989) 1577.
[56] Y.-H. Chiu, H. Fu, J.-T. Huang, S.L. Anderson, J. Chem. Phys. 101 (1994) 5410.
[57] O. Dutuit, C. Metayer, C. Alcarez, P.M. Guyon, D. Gerlich, J. Hepburn, S. Anderson, T. Weng, Proc. SASP'92 (1992) 1.26.
[58] H. Palm, D. Berthomieu, C. Metayer-Zeitoun, C. Alcarez, O. Dutuit, Proc. SASP'94 (1994) 180.
[59] C. Metayer-Zeitoun, C. Alcarez, S.L. Anderson, H. Palm, O. Dutuit, J. Phys. Chem. 99 (1995) 15523.
[60] S.J. Klippenstein, J. Chem. Phys. 104 (1996) 5437.
[61] Q. Cui, Z. Liu, K. Morokuma, J. Chem. Phys. 109 (1998) 56.
[62] S.G. Lias, in: P.J. Linstrom, W.G. Mallard (Eds.), NIST Standard Reference Database Number 69, National Institute of Standards and Technology, Gaithersburg, MD, 2003, http://webbook.nist.gov.
[63] Y.-H. Chiu, B. Yang, H. Fu, S.L. Anderson, J. Chem. Phys. 102 (1995) 1188.
[64] R.J. Green, H.-T. Kim, J. Qian, S.L. Anderson, J. Chem. Phys. 113 (2000) 4158.
[65] H.-T. Kim, J. Liu, S.L. Anderson, J. Chem. Phys. 115 (2001) 1274.
[66] H.-T. Kim, J. Liu, S.L. Anderson, J. Chem. Phys. 115 (2001) 5843.
[67] H.-T. Kim, J. Liu, S.L. Anderson, J. Chem. Phys. 114 (2001) 7838.
[68] H.-T. Kim, J. Liu, S.L. Anderson, J. Phys. Chem. A 106 (2002) 9798.
[69] J. Qian, H. Fu, S.L. Anderson, J. Phys. Chem. A 101 (1997) 6504.
[70] J. Liu, B. Uselman, B.V. Devener, S.L. Anderson, J. Phys. Chem. A 108 (2004) 9945.